S1 Conversion from actual to standard volumetric flow rate

$$(S1)\ Q_{std} = Q_{actual}\frac{P_{actual}T_{std}}{P_{std}T_{actual}}$$

Where Q_{std} is the standard volumetric flow rate in standard liters per minute (SLPM), Q_{actual} is the measured volumetric flow rate in liters per minute (LPM), P_{actual} is the measured pressure (bar), and T_{actual} is the measured temperature (K). P_{std} and T_{std} were taken as 1 bar and 273.15 K - the standard pressure and temperature defined by the international union of pure and applied chemistry (IUPAC; (Ewing et al., 1994).

S2 Contaminants of emerging concern (CECs) analysis

LC separation of Ibuprofen (IBP) was conducted by using a mixture of methanol (MeOH) and 1% (V/V) formic acid (FA) solution as a mobile phase. The gradient program was as follows: constant 50% MeOH and 50% FA solution during 0.5 min, then changes of 50–100% MeOH, 50–0% FA solution were taken in 0.5-8 min. 100% content of MeOH was kept until 10 min and then restored to 50% at 11 min. Constant 50% MeOH and 50% FA solution was kept for 4 min (11-15 min.). Electrospray mass data were acquired in the negative mode with a spray voltage of -4.2 kV. The source temperature was 500°C. N_2 was used as the curtain gas (setting 35), IonSource gas 1 (GS1 gas setting 60) and IonSource gas 2 (GS2 gas setting 40). MS/MS was performed using N_2 as collision gas (CAD gas setting 3). Other specific operating conditions are shown in Table S1.

Table S1. Optimized LC-MS/MS parameters for IBP

	IBP[a]	IBP[b]
[M-1]/Fragment Ion (m/z)	205.1/159.1	205.1/161.1
Delustering potential DP (V)	-18	-18
Entrance potential EP (V)	-10	-10
Collision energy (rel. units)	-15	-15
Collision cell exit potential CXP (V)	-4	-4
Retention time (RT)	10.96	10.96

[a] for quantitation. [b] for qualitative identification.

LC separation of Carbamazepine (CBZ) and Benzotriazole (BTR) was also conducted by using a mixture of methanol (MeOH) and 1% (V/V) formic acid (FA) solution as a mobile phase. The gradient program was as follows: constant 5% MeOH and 95% FA solution for 2 min, then changes of 5–100% MeOH, 95–0% FA solution were taken in 2–7 min. 100% content of MeOH was kept until 11 min and then restored to 5% at 13 min. Constant 5% MeOH and 95% FA solution was kept for 6 min

(13-19 min). Electrospray mass data were acquired in the positive mode with a spray voltage of 5.5 kV. The source temperature was 550°C. N_2 was used as the curtain gas (setting 30), IonSource gas 1 (GS1 gas setting 50) and IonSource gas 2 (GS2 gas setting 60). MS/MS was performed using N_2 as collision gas (CAD gas setting 10). Other specific operating conditions are shown in Table S2.

Table S2. Optimized LC-MS/MS parameters for CBZ and BTR

	CBZ[a]	CBZ[a]	BTR[a]	BTR[b]
[M+1]/Fragment Ion (m/z)	237.1/194.1	237.1/193.1	120.1/65.2	120.1/92.0
Delustering potential DP (V)	40	40	42	42
Entrance potential EP (V)	10.5	10.5	10.5	10.5
Collision energy (rel. units)	25	25	32	23
Collision cell exit potential CXP (V)	4	4	2.5	5.0
Retention time (RT)	10.5	10.5	9.24	9.24

[a] for quantitation. [b] for qualitative identification.

S3 Synthetic effluent composition

Table S3. Basic parameters of the synthetic effluent – mean ± SD

Experiment	[NH$_4^+$] (mg-N L^{-1})	[TKN] (mg L^{-1})	[NO$_3^-$] (mg-N L^{-1})	[TN] (mg L^{-1})	[DOC] (mg L^{-1})
FDO	2.46 ± 0.95	8.94 ± 0.66	1.53 ± 0.37	10.48 ± 0.88	41.61 ± 1.38
AI-LF$_1$	1.83 ± 0.43	9.03 ± 0.21	0.12 ± 0.01	9.16 ± 0.21	41.50 ± 0.99
AI-HF$_1$	3.61 ± 0.49	8.20 ± 0.07	0.66 ± 0.09	8.88 ± 0.11	40.37 ± 1.49
AI-HF$_2$	4.19 ± 0.29	8.42 ± 0.30	0.96 ± 0.41	9.39 ± 0.17	39.82 ± 0.69
AI-HF$_3$	2.96 ± 0.44	7.66 ± 0.79	0.71 ± 0.04	8.37 ± 0.78	40.66 ± 3.35
AI-LF$_2$	3.68 ± 0.51	8.30 ± 0.20	0.81± 0.14	9.12 ± 0.10	42.56 ± 1.59

Table S4. Concentrations of emerging contaminants in the synthetic effluent – mean ± SD

Experiment	[IBP] (μg L^{-1})	[CBZ] (μg L^{-1})	[BTR] (μg L^{-1})
FDO[a]	0.76 ± 0.03	1.66 ± 0.04	7.37 ± 2.24
AI-LF$_1$	1.45 ± 0.08	1.05 ± 0.05	9.48 ± 0.47
AI-HF$_1$	1.06 ± 0.14	0.91 ± 0.07	9.05 ± 0.43
AI-HF$_2$	0.80 ± 0.09	1.08 ± 0.04	8.90 ± 0.44
AI-HF$_3$	71.57 ± 6.97	1.24 ± 0.02	8.43 ± 0.25
AI-LF$_2$	65.00 ± 3.78	2.25 ± 0.08	4.83 ± 0.30

[a] In FDO, samples were taken and analyzed for only one replicate

S4 Volumetric water content (VWC) at various depths during the three main experiments

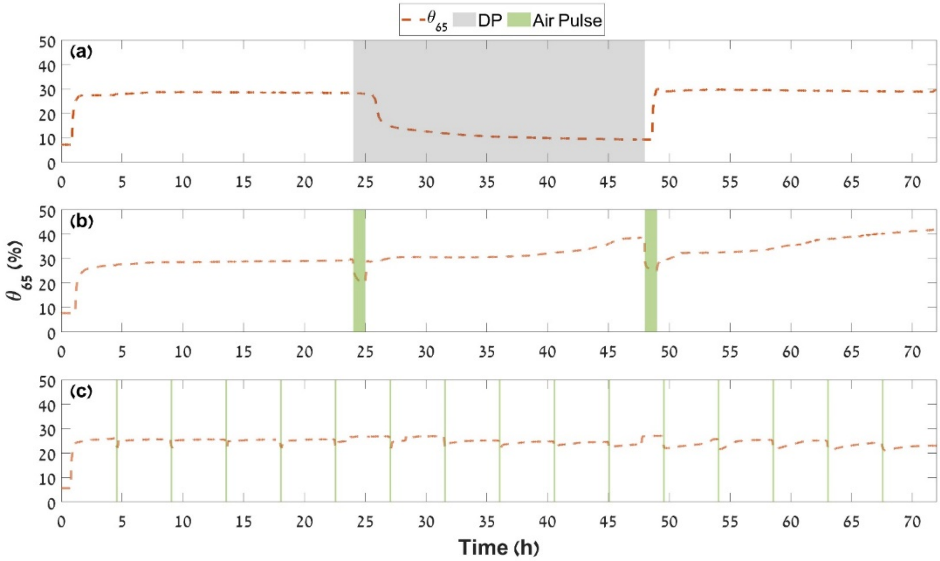

Fig. S1. VWC at a depth of 65 cm below soil surface (θ_{65}) during FDO, AI-LF$_1$ and AI-HF$_1$ (panels **a**, **b** and **c**, respectively). Gray areas symbolize DP, while green areas symbolize the air pulses.

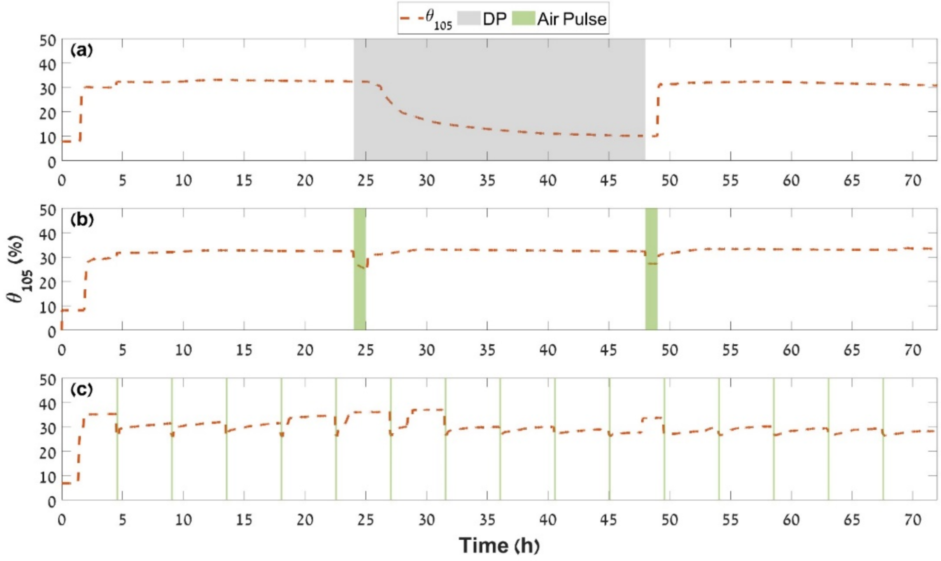

Fig. S2. VWC at a depth of 105 cm below soil surface (θ_{105}) during FDO, AI-LF$_1$ and AI-HF$_1$ (panels **a**, **b** and **c**, respectively). Gray areas symbolize DP, while green areas symbolize the air pulses.

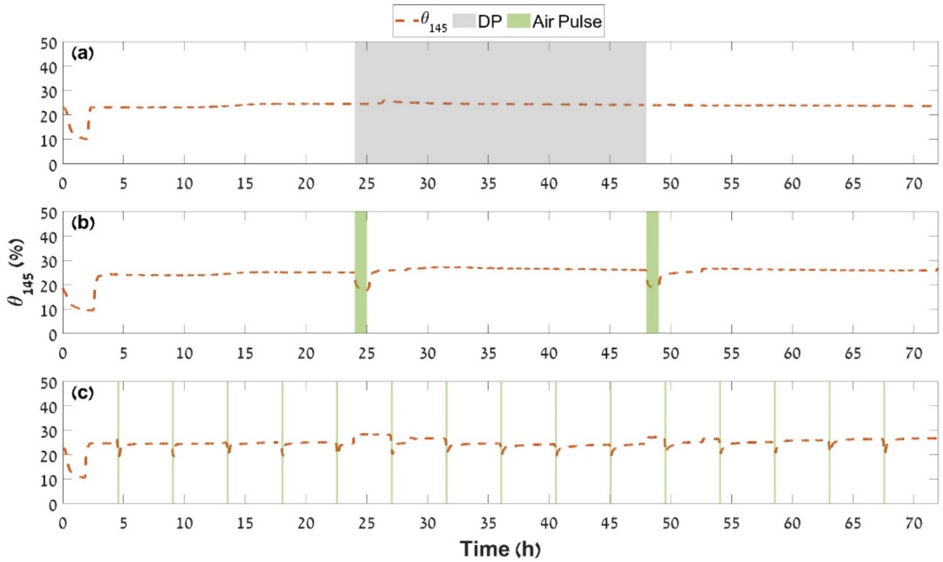

Fig. S3. VWC at a depth of 145 cm below soil surface (θ_{145}) during FDO, AI-LF$_1$ and AI-HF$_1$ (panels **a**, **b** and **c**, respectively). Gray areas symbolize DP, while green areas symbolize the air pulses.

S5 Infiltrated volumes and mean infiltration rates

Table S5. Infiltrated volumes and mean infiltration rates throughout each experiment

Time (h)	0-24	24-48	48-72
Experiment	Infiltrated volume in L (mean infiltration rate in cm h^{-1})		
FDO (1)	95 (20.30)	0 (0)	91 (19.44)
FDO (2)	151 (32.26)	0 (0)	81 (17.31)
AI-LF$_1$	96 (20.51)	132 (28.20)	129 (27.56)
AI-HF$_1$	111 (23.71)	97 (20.72)	67 (14.31)
AI-HF$_2$	92 (19.66)	89 (19.01)	69 (14.53)
AI-HF$_3$	103 (22.01)	71.5 (15.28)	54 (11.54)
AI-LF$_2$	120 (25.64)	112.5 (24.03)	103 (22.01)

S6 Oxidation-reduction potential (ORP) at various depths during the three main experiments

75

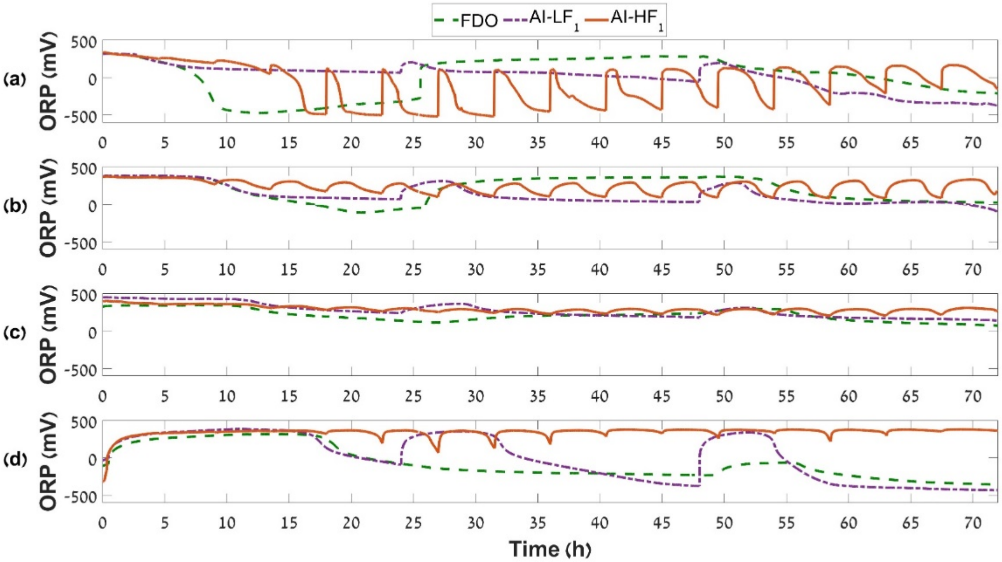

Fig. S4. ORP vs. Ag/AgCl at depths of 25, 65, 105 and 145 cm below soil surface (panels **a**, **b**, **c**, and **d**, respectively) during FDO, AI-LF$_1$ and AI-HF$_1$.

S7 Surface head (SH) during the three main experiments

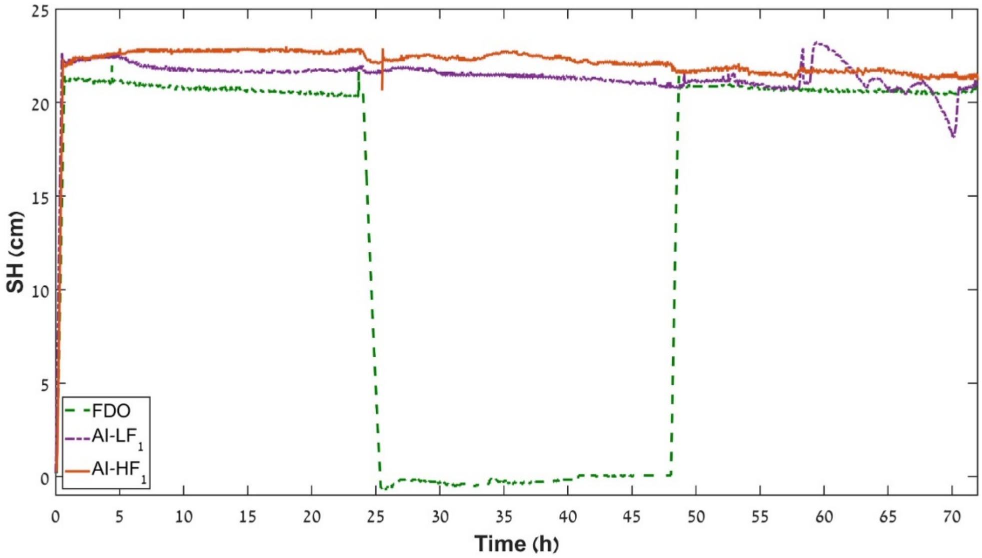

Fig. S5. Surface head (SH) during FDO, AI-LF$_1$ and AI-HF$_1$.

S8 Dissolved oxygen (DO) during the three main experiments

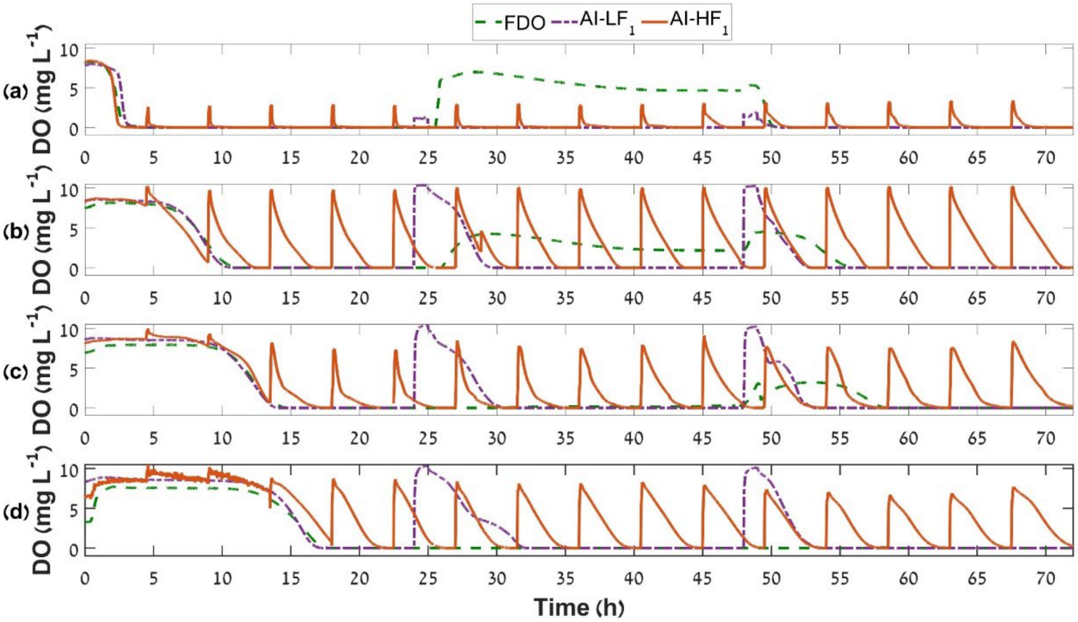

Fig. S6. DO at depths of 25, 65, 105 and 145 cm below soil surface (panels **a**, **b**, **c**, and **d**, respectively) during FDO, AI-LF$_1$ and AI-HF$_1$.

80

S9 Effluent quality

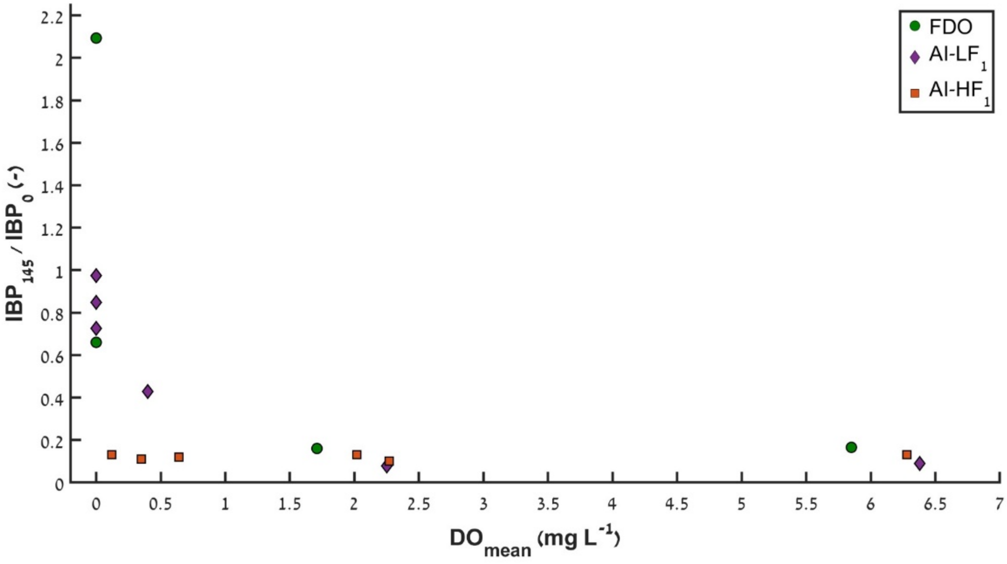

Fig. S7. IBP concentration at a depth of 145 cm vs. the mean DO throughout the column, during FDO, AI-LF$_1$ and AI-HF$_1$. The concentration is normalized to the inlet concentration. Values below detection limit (DL) were regarded with DL/2. In FDO, samples were taken and analyzed for only one replicate

Table S6. Basic parameters of the effluent at a depth of 145 cm, normalized to the inlet concentration – mean ± SD

Experiment	[TKN] (-)	$[NO_3^-]$ (-)	[TN] (-)	[DOC] (-)
FDO	0.51 ± 0.38	0.45 ± 0.74	0.50 ± 0.25	0.14 ± 0.08
AI-LF$_1$	0.62 ± 0.30	2.13± 3.46	0.64 ± 0.28	0.23 ± 0.18
AI-HF$_1$	0.11 ± 0.13	5.63 ± 1.67	0.58 ± 0.13	0.05 ± 0.01
AI-HF$_2$	0.15 ± 0.10	3.30 ± 1.92	0.47 ± 0.20	0.05 ± 0.05
AI-HF$_3$	0.65 ± 0.29	0.57 ± 1.29	0.64 ± 0.18	0.16 ± 0.06
AI-LF$_2$	0.72 ± 0.34	0.26 ± 0.62	0.68 ± 0.25	0.37 ± 0.22

[a] Values below the quantitation limit (QL) were regarded with QL/2.

Table S7. Concentrations of CECs in the effluent at a depth of 145 cm, normalized to the inlet concentration – mean[a] ± SD

Experiment	[IBP] (-)	[CBZ][b] (-)	[BTR][b] (-)
FDO[c]	0.77 ± 0.91	0.91 ± 0.02	0.79 ± 0.33
AI-LF$_1$	0.52 ± 0.39	0.99 ± 0.14	0.99 ± 0.07
AI-HF$_1$	0.12 ± 0.01	0.92 ± 0.13	0.81 ± 0.05
AI-HF$_2$	0.16 ± 0.02	1.00 ± 0.11	0.91 ± 0.09
AI-HF$_3$[d]	0.89 ± 0.02	-	-
AI-LF$_2$	0.84 ± 0.27	0.97 ± 0.03	0.94 ± 0.01

[a] Values below the detection limit (DL) were regarded with DL/2.

[b] The first sample from each experiment (taken at t ~ 4.3 h) was excluded as an outlier since it showed much lower concentrations than the others, apparently due to retardation of CBZ and BTR as a result of their interactions with soil components.

[c] In FDO, samples were taken and analyzed for only one replicate.

[d] For AI-HF$_3$, CBZ and BTR samples were analyzed only at the inflow.

References

Ewing, M. B., Lilley, T. H., Olofsson, G. M., Ratzsch, M. T., and Somsen, G.: Standard quantities in chemical thermodynamics. Fugacities, activities and equilibrium constants for pure and mixed phases (IUPAC Recommendations 1994), Pure Appl. Chem., 66, 533–552, https://doi.org/10.1351/pac199466030533, 1994.